Restricted Rotation Involving the Tetrahedral Carbon. LX. *peri*-Substituent Effect on the Rotational Barrier of the 9-Methyl Group in Several Triptycene Derivatives[1)]

Gaku YAMAMOTO* and Michinori ŌKI†
Department of Chemistry, Faculty of Science, The University of Tokyo, Bunkyo-ku, Tokyo 113
(Received June 19, 1990)

Dynamic ^{1}H NMR study was made on several 1-substituted 8,13-dichloro-9-methyltriptycenes and 8-chloro-13-fluoro-9-methyltriptycenes to examine the effect of the *peri*-substituents on the rotational barrier of the 9-methyl group. The rotational barrier height increases in the expected order as the 1-hydrogen is replaced by a bulkier group up to CH_3, but shows a very low value when a *t*-butyl group is introduced into 1-position to show that destabilization of the ground state by the bulky *t*-butyl group exceeds that of the transition state for rotation.

In 1973, we reported the first observation of restricted rotation of a methyl group by dynamic NMR spectroscopy:[2a)] the 9-methyl proton signal in 1,2,3,4,5,6,7,8-octachloro-9-methyltriptycene (**1**) comprised a two-proton doublet and a one-proton triplet at −72 °C, which coalesced into a singlet at a higher temperature, the lineshape analysis affording a value of 13.5 kcal mol^{-1} (1 cal$_{th}$=4.184 J) as the enthalpy of activation for the internal rotation of the 9-methyl group.

Subsequently we studied the rotational barriers of several 9-methyltriptycene derivatives with various substituents at *peri*-positions of the triptycene skeleton.[3)] Among several intriguing features, a higher barrier was suggested for 1,4-dimethoxy-9-methyltriptycene (**2**) than for 1,4,9-trimethyltriptycene (**3**). This seemed to contradict the prediction from the generally accepted order of the bulkiness of the groups, CH_3>OCH_3. We offered a hypothesis that gearing of the 1- and 9-methyl groups might be responsible for the low barrier in **3**, which suffered some criticism.[4)] The inference, however, was somewhat inconclusive because the slow exchange limit spectra were not observed for these compounds and the argument was made on the basis of the signal widths.[3)]

Later, we showed definite experimental evidence that in singly *peri*-substituted 9-(1,1-dimethyl-2-phenylethyl)triptycenes (**4**)[5a,b)] and 9-isopropyltriptycenes (**5**)[5c)] the *peri*-methoxyl compound has a higher barrier to rotation of the 9-substituent than the *peri*-methyl one: the general tendency is that the rotational barrier at first increases and then decreases as the *peri*-substituent becomes bulkier, and thus a plot of the rotational barrier against the bulkiness of the *peri*-substituent looks inversely V-shaped. The *peri*-fluorine compound is at the apex in the *t*-alkyl series and the *peri*-methoxyl one is there in the *s*-alkyl series (Fig. 1). This fact was ascribed to the greater destabilization of the ground state relative to the transition state for rotation upon introduction of a bulky *peri*-substituent.[5)]

These findings prompted us to make a more systematic study of the *peri*-substituent effect on the rota-

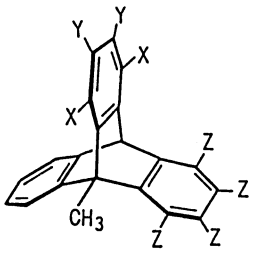

	X	Y	Z
1	Cl	Cl	Cl
2	OCH_3	H	H
3	CH_3	H	H
16	CH_3	H	Cl

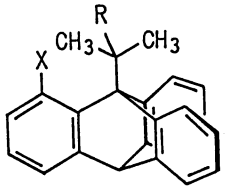

4 R=$CH_2C_6H_5$
5 R=H

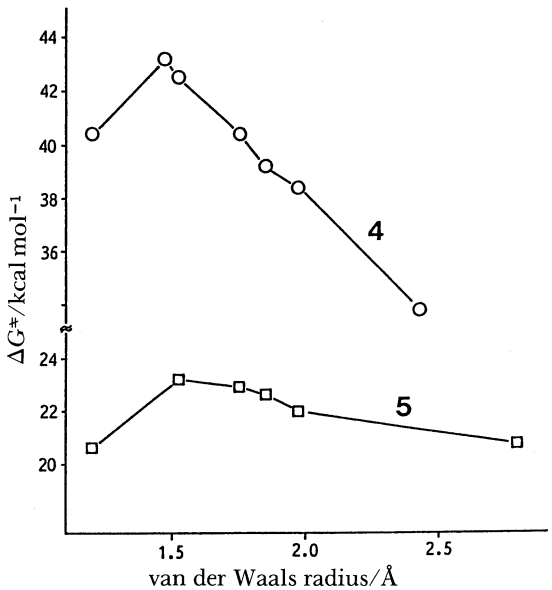

Fig. 1. Dependence of the rotational barriers in **4** and **5** on the sizes of the *peri*-substituents.

† Present address: Department of Chemistry, Faculty of Science, Okayama University of Science, Ridaicho, Okayama 700.

tional barrier of the 9-methyl group in 9-methyltriptycene derivatives. In order to raise the rotational barriers so as to be fully studied by dynamic NMR, we introduced two chloro groups at two of the *peri*-positions and hence examined compounds **6a—f**. Furthermore, we included two additional compounds **7a** and **7b** with a fluoro group instead of Cl at one of the *peri*-positions. The results are described and discussed in this article, especially in connection with the correlation between the sizes of the substituents and the effects on the rotational barriers.

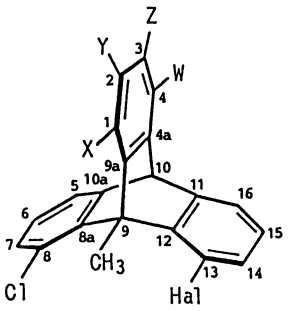

	Hal	X	Y	Z	W
6a	Cl	H	H	H	H
6b	Cl	F	F	F	F
6c	Cl	OCH_3	H	H	OCH_3
6d	Cl	CH_3	H	H	CH_3
6e	Cl	$C(CH_3)_3$	H	$C(CH_3)_3$	H
6f	Cl	H	$C(CH_3)_3$	H	$C(CH_3)_3$
6g	Cl	Br	Br	Br	Br
7a	F	OCH_3	H	H	OCH_3
7b	F	CH_3	H	H	CH_3

During the course of this study we found very interesting phenomena in the long-range ^1H-^{19}F spin-spin couplings in the fluorine-containing compounds, **6b**, **7a**, and **7b**, which are also discussed.[6]

Results

Synthesis. Commercially available 1,8-dichloroanthraquinone (**8**) was treated with caesium fluoride in dimethyl sulfoxide to give 1-chloro-8-fluoroanthraquinone (**9**), which was chemoselectively reduced to 1-chloro-8-fluoroanthrone (**11**) by treatment with aluminium powder in concentrated sulfuric acid, just as **8** was chemoselectively converted to 1,8-dichloroanthrone (**10**).[7] The anthrones **10** and **11** were treated with methylmagnesium iodide followed by dehydration to give 1,8-dichloro- (**12**)[8] and 1-chloro-8-fluoro-9-methylanthracene (**13**), respectively.

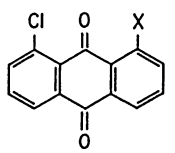

8: X=Cl
9: X=F

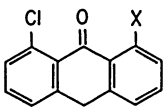

10: X=Cl
11: X=F

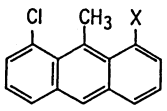

12: X=Cl
13: X=F

Reactions of the anthracenes **12** and **13** with appropriate benzynes afforded the triptycenes **6a**, **6b**, **6d—f**, and **7b**. Addition of 3,5-di-*t*-butylbenzyne to **12** afforded **6e** and **6f** in a ratio of ca. 2:5. The structures of **6e** and **6f** were assigned on the basis of the chemical shift values of 10-H. The 10-H in **6f** suffers from strong steric compression by the 4-*t*-butyl group and give the signal at a very low field of δ=6.07 while that in **6e** resonates at a similar position as that in **6a** (Table 4). The assignments were further confirmed by the nuclear Overhauser effect (NOE) experiments; in **6e** irradiation of 10-H at δ=5.20 enhanced the doublet signal at δ=7.21 assignable to 4-H as well as the signal due to 5/16-H, while in **6f** irradiation of the 4-*t*-butyl signal at δ=1.55 enhanced the 10-H signal at δ=6.07 together with the 3-H signal at δ=7.15. Predominant formation of the less crowded isomer **6f** is of interest because usually the more crowded regioisomer is preferentially formed in the Diels-Alder reaction of unsymmetrical benzynes.[9] Reactions of **12** and **13** with *p*-benzoquinone followed by aromatization and *O*-methylation gave **6c** and **7a**, respectively. Synthesis of the 1,2,3,4-tetrabromo derivative **6g** was tried by addition of tetrabromobenzyne to **12** but the product supposed to be **6g** had extremely low solubility in common solvents and the purification and characterization of **6g** was abandoned.

^{1}H NMR Spectra. ^{1}H NMR spectral data of the triptycenes **6** and **7** obtained at 25 °C in $CDCl_3$ at 500 MHz are given in Table 4. In the compounds other than the 1,4-dimethoxyl derivatives **6c** and **7a**, all the signals could be unambiguously assigned with the aid of homonuclear decoupling and NOE experiments. In **6c** and **7a** two methoxyl signals are too close to be definitely assigned. The 9-methyl signal is considerably broadened in all of the compounds at 25 °C, since the internal rotation of the 9-methyl group is slowed down to some extent on the NMR time scale. The 9-methyl protons of **6b** and **7b** give a broad singlet at 500 MHz and 25 °C, but a broad doublet with the splitting of 7.0 Hz due to coupling with *peri*-F at 90 MHz and 35 °C.

Low temperature spectra of the triptycenes were obtained in CD_2Cl_2. On lowering the temperature, the 9-methyl signal decoalesced into a multiplet except for **6c**, in which the signal remained a rather sharp singlet down to −90 °C because of the very small chemical shift difference between the diastereotopic protons. For the other compounds, slow exchange limit spectra were observed at −70 °C except for **6e**, which did not completely reach the slow-exchange limit even at −115 °C, the lowest attainable temperature, because of the low barrier to rotation. At the lowest temperatures the 9-methyl signal appeared as an AB_2 pattern in **6a** and **6d—f**, and as an AB_2 part of an AB_2X spectrum in **6b**. In **7b** the signal appeared

as an ABC part of an ABCX pattern at −70 °C, while in **7a** that looked like an AB_2 part of an AB_2X spectrum because of the coincidence of the two chemical shifts.

The 9-methyl signal of **6c** remained singlet down to −90 °C in acetone-d_6 as well, but in toluene-d_8 it decoalesced below about −25 °C and appeared as an AB_2 pattern with the chemical shift difference of about 0.08 ppm at −65 °C.

The slow exchange limit spectra of **6** and **7** were iteratively simulated using the LAOCN3 program[10] to obtain the NMR parameters, which are given in Table 1. Assignments were easily made for compounds **6** by the relative intensities and the coupling pattern. As for **7a** and **7b**, the assignments were made by assuming the additivity of the *peri*-substituent effects on the chemical shifts, as discussed in the later section in detail.

Lineshapes of the exchange-broadened spectra in the intermediate temperature ranges were simulated using the DNMR3 program[11] to obtain the rate constants for the internal rotation of the 9-methyl group. The rate constants were obtained at six to ten temperatures in the range of ca. 40 degrees for each compound. Least-squares analyses of Eyring plots of the rate constants afforded the kinetic parameters given in Table 2. The errors in the kinetic parameters for **6e** are somewhat larger than for the other compounds because of the narrower temperature range in which the lineshape analysis could be made.

^{13}C NMR Spectra. ^{13}C NMR spectra of the triptycenes were measured at 25 °C in $CDCl_3$ and the data are given in Table 5. Assignments were made on the basis of off-resonance decoupled and ^{1}H-coupled spectra and ^{1}H-^{13}C COSY spectra as well as comparison with the reported data for triptycene derivatives.[12] Couplings with ^{19}F were also helpful in case of the fluorine-containing compounds, **6b**, **7a**, and **7b**.

Table 1. NMR Parameters[a]

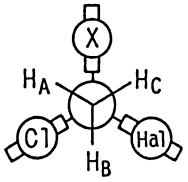

Compd	X	Hal	δ_A	δ_B	δ_C	J_{AB}	J_{AC}	J_{BC}	J_{AF}	J_{BF}	J_{CF}
6a	H	Cl	2.75	3.70	2.75	12.6		12.6			
6b	F	Cl	3.02	3.46	3.02	12.6		12.6	6.1	8.7	6.1
6c[b]	OCH_3	Cl	3.25	3.25	3.25						
			(3.79	3.87	3.79	11.3		11.3)[c]			
6d	CH_3	Cl	3.24	3.42	3.24	12.9		12.9			
6e[d]	*t*-Bu	Cl	3.55	3.35	3.55	13.5		13.5			
6f	H	Cl	2.77	3.70	2.77	12.6		12.6			
7a[e]	OCH_3	F	3.26	2.95	2.95	12.3		12.3	9.0	6.2	6.2
7b	CH_3	F	3.27	3.11	2.95	13.1	11.9	13.1	8.6	6.3	6.3

a) Measured at −70 °C in CD_2Cl_2 unless otherwise stated. Parameters were obtained by simulation using LAOCN3. Coupling constants are in Hz and reliable to ±0.3 Hz. b) No splitting was observed. c) Measured at −65 °C in toluene-d_8. d) Measured at −110 °C in CD_2Cl_2. e) Simulation assumed the magnetic equivalence of H_B and H_C.

Table 2. Kinetic Parameters for the Internal Rotation of the 9-Methyl Groups

Compd	$\Delta H^{\ddagger}$	$\Delta S^{\ddagger}$	$\Delta G^{\ddagger}_{250K}$[a]	k_{250K}	Solv[b]	Field	Temp range[c]	Points
	kcal mol^{-1}	cal mol^{-1} K^{-1}	kcal mol^{-1}	s^{-1}		MHz	°C	
6a	10.9±0.2	0.2±1.0	10.9	1600	A	400	−20—−66	10
6b	13.4±0.3	3.4±1.1	12.5	57	A	270	0—−30	6
6c	13.6±0.6	4.2±2.3	12.6	54	B	500	−4—−38	7
6d	14.1±1.3	4.1±5.0	13.1	20	A	270	0—−30	6
6e	9.5±2.5	2.5±11.9	8.8[d]	98000	A	270	−86—−101	4
6f	11.8±0.2	1.2±0.8	11.5	440	A	270	−15—−61	9
7a	12.1±0.4	3.6±2.0	11.2	760	A	270	−20—−61	9
7b	13.1±0.5	4.0±2.2	12.1	150	A	270	−10—−49	9
1[e]	13.5±0.6	9.8±3.0	11.1	1100	C	100		
16[e]	12.1±0.3	3.0±1.4	11.4	620	C	100		

a) Reliable to ±0.1 kcal mol^{-1} unless otherwise stated. b) A: CD_2Cl_2, B: toluene-d_8, C: $CDCl_3$–CS_2 (8:1). c) The temperature range where the lineshape analysis was made. d) Reliable to ±0.2 kcal mol^{-1}. e) Ref. 3.

Molecular Mechanics Calculations. In order to obtain some insights into the geometries and the energies of the triptycenes in both the ground and transition states, molecular mechanics calculations were performed. The BIGSTRN-3 program[13] with the MM2 force field and the full-matrix Newton-Raphson optimization procedure was used because not only ground states but also transition states can be directly optimized as stationary points with zero and one imaginary force constant, respectively. Several of the original MM2 force-field parameters were modified and some were added as described in the Experimental section. The calculated rotational barriers of the 9-methyl groups obtained as the steric energy differences between the ground and transition states as well as their components are given in Table 3.

Discussion

Rotational Barriers. In discussing the effects of substituents on rotational barriers, not only those on the transition state energy but also those on the ground state one should be considered. Although the effect on the ground state has often been neglected or treated lightly, our studies on 9-*t*-alkyl- and 9-*s*-alkyltriptycenes[5] clearly demonstrated the importance of this notion. In these compounds the destabilizing effects, mostly steric in origin, of the *peri*-substituent on the ground state are sometimes greater than those on the transition state, resulting in the decrease in the rotational barrier with increasing bulkiness of the *peri*-substituent (Fig. 1). In the present case of 9-methyltriptycene derivatives, the *peri*-substituent effects, especially those on the ground state, are expected to be much smaller than in the 9-*t*-alkyl or 9-*s*-alkyl cases, because the 9-methyl group is far less bulky.

The rotational barriers as expressed in terms of the free energies of activation at 250 K in the 1-substituted 8,13-dichloro series **6** show the order of *t*-Bu$\ll$H$<$F$\approx$OCH$_3<$CH$_3$, if the solvent effect is ignored (Table 2). If the *peri*-*t*-butyl compound **6e** is excluded, the barrier height increases with the generally accepted order of the bulkiness of the *peri*-substituent. This implies that the *peri*-substituent effect on the ground state is less important than that on the transition state in this range of *peri*-group bulkiness.

When a *t*-butyl group is introduced at a *peri*-position, the barrier height decreases to a great extent. The ground state is significantly destabilized because of large steric congestion, while the transition state for rotation is destabilized to a lesser extent than the ground state, resulting in the low barrier to rotation, even lower than that in **6a**. Therefore, an inversely V-shaped plot of the barrier vs. the bulkiness of the *peri*-substituent is drawn also in the 8,13-dichloro-9-methyltriptycene series.

Several remarkable features will be discussed in the following paragraphs. The *peri*-methyl compound **6d** has a higher barrier than the *peri*-methoxyl compound **6c**. The same trend is also observed in the 8-chloro-13-fluoro series, **7a** and **7b**. These results may be reasonable because a "positive" correlation between the barrier and the size of the *peri*-substituent holds in this region. As this correlation is expected to hold also in the less congested 9-methyltriptycenes with a single *peri*-substituent, the earlier suggestion[3] that **2** would have a higher barrier than **3** must have been an artifact probably because of the difference between **2** and **3** in the chemical shift differences between the diastereotopic protons. This point will be discussed further in the later section.

Compound **6a** shows a slightly lower barrier than the octachloro derivative **1**,[2,3] i.e., the small "positive" buttressing effect is observed:[5b] an effectively bulkier *peri*-group gives a higher barrier. Although this is not conclusive because these two data are not of the same quality, if this is true, the barrier-bulkiness plot should have a maximum at a compound with a bulkier *peri*-substituent than Cl.

Comparison of the data for **6b** and **7b** together with a reasonable assumption that the buttressing effect in the tetrafluoro compound is negligible[5b] indicates that Cl has a larger effect on the barrier than CH$_3$. Imashiro et al. reported that **14** with *peri*-chloro groups has a higher barrier than **15** with *peri*-methyl groups both in the solid state and in solution.[14c] Usually, CH$_3$ is thought to be bulkier than Cl, as inferred by the van der Waals radii of 2.0 and 1.8 Å for CH$_3$ and Cl, respectively.[15] One interpretation for this may be that the apex exists between Cl and CH$_3$. In order to check this point further, examination of the *peri*-bromo compound **6g** was tried without success as mentioned in the introductory and experimental sections.

In the comparative discussion above, we have implicitly assumed that the geometry of the triptycene skeleton does not change from compound to compound and that the change in the barrier height depends solely on the nature of the *peri*-substituent. We must however admit that this is simply a first approximation. This is suggested by the fact that the 2,4-di-*t*-butyl compound **6f** has a somewhat higher barrier than **6a**. This may be explained in terms of the buttressing effect of the 2-*t*-butyl group toward the 1-hydrogen. We prefer, however, the explanation that the *t*-butyl groups cause a considerable change in the geometry of the triptycene skeleton, which results

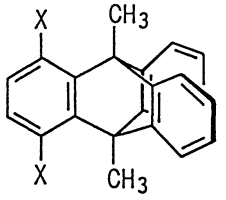

14 X=Cl
15 X=CH$_3$

Table 3. Calculated Rotational Barriers and Their Components (kcal mol^{-1})

	6a	**6b**	**6c**	**6d**	**6e**	**6f**	**7a**	**7b**
Total	12.688	14.232	15.684	14.458	8.706	13.959	14.105	13.558
Bond	2.090	2.544	1.260	0.777	0.599	2.413	2.312	1.694
Angle	4.960	5.461	6.253	5.824	4.978	5.197	5.355	5.260
Torsional	0.814	0.608	4.846	5.643	1.886	0.808	1.150	2.430
Nonbonded	4.619	5.271	3.094	2.079	1.177	5.367	5.116	3.996
Dipole	0.055	0.192	0.082	0.047	0.041	0.020	0.018	0.055
Str-Bend	0.136	0.147	0.078	0.006	−0.021	0.115	0.138	0.087

in the difference between **6a** and **6f**.

We may conclude that an inversely V-shaped plot of the barriers vs. the bulkiness of the *peri*-substituents can be observed in any series of *peri*-substituted 9-alkyltriptycene derivatives. As the steric interaction between the *peri*- and the bridgehead groups increases, both the ground state and the transition state are destabilized. When the interaction is small, the transition state destabilization upon replacement of the *peri*-group by a bulkier one exceeds that of the ground state, resulting in the increase of the barrier. If the steric interaction becomes extremely large beyond some critical point, the destabilization of the ground state becomes larger than that of the transition state, resulting in the decrease of the barrier.

We believe that substituent steric effects of this tendency are generally observed in any internal rotation system. That is, we should not expect that the order of the bulkiness of the substituents is always reflected in the order of the rotational barriers about a single bond, of which at least one end is an sp^3-hybridized carbon.[16]

Molecular Mechanics Calculations. Several attempts to reproduce the rotational barriers in triptycene derivatives by molecular mechanics calculations have been reported using the bond drive technique.[14,17] In every case the calculated barriers had been considerably higher than the experimental ones. Recently Imashiro et al.[14c] reported that the rotational barrier in **15** could well be reproduced by employing the MM2′ force field and the torsional parameter V_3 of zero for C(sp^2)-C(sp^3)-C(sp^3)-H. The calculated barrier was 10.01 kcal mol^{-1}, while the experimentally obtained enthalpy of activation in CD_2Cl_2 was 9.05 kcal mol^{-1}.

The results of the molecular mechanics calculations for triptycenes **6** and **7** given in Table 3 reproduce the general trends of the experimental data, though the absolute values are again generally higher than the observed. Especially the very low barrier of **6e** is well reproduced. One of the discrepancies is that the calculated barriers of the *peri*-methoxyl compounds **6c** and **7a** are higher than the corresponding *peri*-methyl compounds **6d** and **7b**, respectively. Inadequacy of the force field parameters should at least partly be responsible.

As for the ground state geometries, all the molecules in series **6** except for **6e** exist in a conformation with C_s symmetry. Molecules of **6e** exist as a chiral C_1 conformation with somewhat distorted triptycene skeleton, although the C_s conformation lies only 0.05 kcal mol^{-1} above the C_1 conformation, constituting the saddle point connecting the enantiomeric C_1 forms. At the transition state for the 9-methyl group rotation, all the molecules of series **6** adopt a C_s conformation.

As the component analysis in Table 3 shows, the angle strain and nonbonded strain terms are important in all compounds. The torsional strain term makes a significant contribution when the rotational barrier is high as in **6c** and **6d**, reflecting a large distortion of the triptycene skeleton at the transition state in these compounds.

9-Methyl Proton Chemical Shifts. Careful examination of the chemical shift data of the 9-methyl protons (Table 1) reveals several intriguing features. In compounds **6**, the 9-methyl protons gauche or synclinal to the *peri*-substituent X (H_{sc}) give the signal at a lower field as X becomes bulkier probably because of the field/anisotropy effect and steric compression effect of X. On the other hand, the signal due to the proton antiperiplanar to X (H_{ap}) shifts upfield as X is changed from hydrogen to another group. Therefore, X has a significant influence not only on the proximate protons (H_{sc}) but also on the remote proton (H_{ap}). This point will be further discussed later in this paper.

We can make assignments for the 9-methyl protons in **7a** and **7b** by assuming that the substituent effects are additive and that the *peri*-substituent exerts the same magnitude of the effect on both of the *sc*-protons. Thus the chemical shift difference between H_B and H_C in **7a** should be the same as that in **6c**, i.e., $\delta_B-\delta_C=3.25-3.25=0$, and the difference in **7b** should be the same as that in **6d**, i.e., $\delta_B-\delta_C=3.42-3.24=0.18$ ppm. The chemical shift difference between H_A and H_B may be estimated by summing up the *peri*-substituent effects relative to *peri*-H according to the following equation: $\delta_A-\delta_B=[(3.25-2.75)+(3.46-3.70)]-[(3.25-3.70)+(3.02-2.75)]=0.44$ ppm for **7a** and $[(3.24-2.75)+(3.46-3.70)]-[(3.42-3.70)+(3.02-2.75)]=0.26$ ppm for **7b**. Therefore, in **7a**, H_B and H_C are expected to resonate at the same position and H_A appears at a lower field than these, while in **7b**, H_A

will be at the lowest field and H_C at the highest field. The assignments according to this prediction are given in Table 1. Although the absolute values of the observed chemical shift differences are somewhat different from the prediction, the results are highly consistent.

This simple additivity rule also predicts that the chemical shift difference between the diastereotopic protons in the 9-methyl group of **2** should be larger than that in **3** by ca. 0.2 ppm, contrary to the previous prediction that both compounds would have similar chemical shift differences.[3] This may explain why the 9-methyl signal of **2** was broader than that of **3** at low temperatures.[3]

Long-Range ^{1}H-^{19}F Coupling and Charge Transfer.[6] In **6b**, **7a**, and **7b** where a fluoro group is at a *peri*-position, long-range ^{1}H-^{19}F couplings are observed between the fluorine nucleus and the 9-methyl protons: in the spectra at the slow-exchange limit, the diastereotopic protons of the 9-methyl group couple separately with the *peri*-F (Table 1). That the coupling partner in **6b** is actually 1-F is deduced not only by the quite similar behavior of **7a** and **7b** but also by the careful analysis of the ^{19}F spectrum of **6b**. Although the 1-F signal appears as an unresolvable multiplet, the other fluorine signals are easily analyzed by a first-order approximation which indicates that 2-F, 3-F, and 4-F do not couple with proton(s).

The absolute signs of the ^{1}H-^{19}F coupling constants are yet uncertain, but the magnitude of 7.0 Hz observed at 25 °C, which should be the weighted average of the respective values at low temperatures, clearly indicate that they are of the same sign.[18]

The fact that the remote proton (H_B in **6b** and H_A in **7a** and **7b**, hereafter referred to as H_{ap}) shows a larger coupling constant than the proximate protons (H_A in **6b** and H_B and H_C in **7a** and **7b**, hereafter H_{sc}) is quite intriguing. Close proximity of *peri*-F and the 9-methyl carbon as well as the nearly linear arrangement of F···C-H_{ap}(ca. 160° by MM2) suggests that the interaction between the lone pair orbital on the fluorine and the rear lobe of the C-H bond orbital should be responsible for the large coupling of H_{ap} with *peri*-F.[19]

In the ^{13}C NMR spectrum of either **6b**, **7a**, or **7b** at ambient temperature, the 9-methyl carbon shows a coupling of 11.9—12.3 Hz with the *peri*-fluorine while the 9-carbon shows a far smaller coupling (<3.9 Hz), if any. This indicates that the couplings exhibited by the 9-methyl carbon and protons are actually through-space in nature, and further confirms that the electrons belonging to the methyl carbon orbitals participate in the F-H_{ap} coupling.[6]

After establishing the through-space interaction between the *peri*-F and the *ap*-C-H group, we can come back to the problem of chemical shifts of the 9-methyl protons. As mentioned earlier, the low-field shifts of the H_{sc}'s can at least partly be attributed to the van der Waals (steric compression) shift, because the *peri*-substituent and H_{sc} are placed in proximity. Under sterically congested circumstances, other nuclei bonded to the atom carrying the protons which suffer

Table 4. ^{1}H NMR Spectral Data (500 MHz) of **6** and **7** at 25 °C in $CDCl_3$[a]

Proton	**6a**	**6b**	**6c**	**6d**	**6e**	**6f**	**7a**	**7b**
9-CH_3	3.094 bs	3.251 bs	3.293 bs	3.334 bs	3.550 s	3.098 bs	3.103 bd (7.0)	3.141 bs
10	5.294 s	5.638 d (1.6)	5.778 s	5.518 s	5.200 s	6.068 s	5.812 d (2.0)	5.551 d (2.0)
1	7.509 d (7.6)		3.757 s[b]	2.681 s	1.595 s	7.472 d (1.6)	3.756 s[b]	2.674 s
2	7.116 dt (1.3, 7.5)		6.581 d (8.9)	6.701 d (7.8)	7.319 d (2.1)	1.293 s	6.581 s	6.688 d (7.8)
3	7.094 dt (1.1, 7.3)		6.595 d (8.9)	6.765 d (7.8)	1.263 s	7.150 d (1.6)	6.581 s	6.752 d (7.8)
4	7.378 dd (1.3, 7.2)		3.808 s[b]	2.467 s	7.212 d (2.1)	1.554 s	3.806 s[b]	2.462 s
5	7.240 dd (1.2, 7.2)	7.297 dd (1.2, 7.2)	7.265 dd (1.0, 7.6)	7.229 dd (1.3, 7.2)	7.187 dd (1.3, 7.2)	7.267 dd (1.2, 7.2)	7.265 dd (1.3, 7.3)	7.225 dd (1.3, 7.2)
6	6.885 dd (7.2, 8.0)	6.979 dd (7.2, 8.2)	6.890 t (7.6)	6.895 dd (7.2, 8.0)	6.910 dd (7.2, 8.0)	6.890 dd (7.2, 8.0)	6.877 dd (7.3, 8.0)	6.877 dd (7.2, 8.1)
7	6.985 dd (1.2, 8.0)	7.090 dd (1.2, 8.2)	7.002 dd (1.0, 8.0)	7.006 dd (1.3, 8.0)	7.012 dd (1.3, 8.0)	6.994 dd (1.2, 8.0)	6.989 dd (1.3, 8.0)	6.990 dd (1.3, 8.1)
14							6.702 ddd (1.1, 8.3, 12.4)	6.702 ddd (1.1, 8.2, 12.5)
15							6.957 ddd (4.4, 7.2, 8.3)	6.961 ddd (4.4, 7.2, 8.2)
16							7.163 dd (1.1, 7.2)	7.128 dd (1.1, 7.2)

a) Numbering of the protons corresponds to that shown in the structural formula **6** and **7**. In parentheses are coupling constants in Hz and are reliable to ±0.3 Hz. b) Interchangeable.

Table 5. ^{13}C NMR Spectral Data of **6** and **7** at 25 °C in $CDCl_3$[a)]

Carbon	6a	6b	6c	6d	6e	6f	7a	7b
1	122.69	145.13 ddd*1 (4.0, 12.3, 254.0)	148.43*1	129.56*1	141.87*1	118.15	148.58*1	129.65*1
2	125.44*1	138.32 dddd (3.0,*2 13.3, 17.2, 253.5)	110.10*2	130.95	122.99	143.46*1	110.00*2	130.65
3	125.69*1	138.95 dddd (3.4,*2 12.3, 19.7, 250.5)	111.66*2	127.35	147.22*1	119.90	111.60*2	127.21
4	123.05	141.83 brdd*1 (10.8, 243.4)	151.74*1	130.43*1	119.56	140.26*1	151.63*1	130.22*1
4a	144.83	128.64 td (3.0, 17.2)	134.75	143.43	147.36	147.44	134.89	143.41
9a	147.02	129.20 d (8.8)	136.00	144.46	148.44	149.19	136.19	144.65
5	122.41	122.91	122.59	122.36	122.20	122.26	122.65	122.44
6	126.68	127.49	126.60	126.75	126.88	126.54	126.44	126.58
7	129.57	130.72	129.90	130.08	130.20	129.50	129.61	129.76
8	130.31	130.88	130.47	132.04	130.36	130.25	130.27	131.82
8a	141.39	140.76	142.71	142.41	142.55	142.39	142.83	142.54
10a	149.50	147.18	149.39	149.17	149.81	149.33	149.62	149.41
11							149.52 d (4.0)	149.28 d (4.0)
12							133.14 d (10.0)	132.88 d (9.5)
13							159.29 d (250.8)	159.31 d (250.3)
14							114.58 d (25.9)	114.69 d (26.4)
15							127.19 d (8.5)	127.38 d (8.8)
16							119.31 d (3.3)	119.06 d (3.0)
9	54.11	55.82 br	57.14	58.46	58.03	53.05	54.63 d (3.9)	56.05 d (3.7)
10	55.57	47.50 br	48.47	52.36	58.53	54.44	47.94 d (1.7)	51.78 d (1.9)
9-CH_3	21.31	22.96 d (12.3)	24.37	25.65	27.39	22.00	22.36 d (11.9)	23.62 d (12.3)
1-R			56.37*3	24.12	35.31 p 34.51 q*2		56.41*3	23.61
2-R						31.58 p*2 35.01 q*3		
3-R					31.28 p 36.56 q*2			
4-R			56.67*3	18.76		31.76 p*2 35.56 q*3	56.71*3	18.82

a) Numbering of the carbons corresponds to that shown in the structural formula **6** and **7**. In parentheses are coupling constants with ^{19}F nuclei (Hz) and are reliable to ±0.6 Hz. Values indicated by *1, *2, and *3 are interchangeable within each pair.

the van der Waals shift are known to move upfield.[20)] Thus the upfield shifts of H_{ap} can partially be attributed to this effect. However, if it were the exclusive reason for the upfield shift of the H_{ap}, the order of the upfield shift of the H_{ap} signals in **6b—d** is expected to be CH_3>CH_3O>F, which disagrees with the observed.

As another factor for the origin of the observed results, the charge-transfer interaction between the *n*-orbital of the *peri*-substituent and the C-H_{ap} σ^* orbital is considered. This type of interaction has been established in several triptycene derivatives,[21,22)] and will take place in the present case as well due to the efficient overlap of the relevant orbitals, though weak because of the high-lying σ^* orbital of the C-H bond, to increase the electron density at H_{ap}. The methoxyl group, being most electron-donating and being of a medium size, shifts the H_{ap} resonance to the highest field among the three compounds (**6b—d**), and the methyl group, having no available *n*-electrons but giving the largest congestion effect, places the H_{ap} chemical shift at the middle. The fluoro group, being hardly electron-donating and small, shifts the H_{ap} resonance at the lowest among the compounds.

The behavior of the 9-methyl proton chemical shifts in the *peri-t*-butyl compound **6e** may also be explained in terms of the steric compression effect. ^{13}C NMR spectral data in Table 5 clearly demonstrate the congestion effect, as is known that ^{13}C NMR reflects this effect more effectively than ^{1}H NMR.[23)] These data supplement the discussion given above.

Experimental

Melting points are not corrected. ^{1}H NMR spectral data at ambient temperature were obtained on a Bruker AM-500 spectrometer operating at 500.14 MHz in the pulse FT mode unless otherwise stated. Where indicated as 90 MHz, they were obtained on a Varian EM-390 spectrometer operating at 90.0 MHz in the CW mode. The solvent was $CDCl_3$ unless otherwise stated. Variable temperature ^{1}H NMR spectra were obtained in CD_2Cl_2 or in toluene-d_8 on a Bruker AM-500, a JEOL GX-400 or a JEOL GX-270 spectrometer operating at 500.14, 399.65 or 270.17 MHz, respectively, in the pulse FT mode. The temperatures were calibrated using a methanol sample with AM-500 and GX-270, but

were read as digital outputs without calibration with GX-400. ^{13}C NMR spectra were recorded on AM-500 operating at 125.76 MHz in $CDCl_3$ at 25 °C. ^{19}F NMR spectra were obtained as $CDCl_3$ solutions on a Varian EM-390 spectrometer operating at 84.67 MHz in the CW mode, and the chemical shifts are expressed in ppm downfield from the internal hexafluorobenzene. Gel permeation chromatography was performed on an LC-09 Liquid Chromatograph of Japan Analytical Instruments Co., Ltd. using a series of JAIGEL 1H and 2H columns and chloroform as the eluent.

1-Chloro-8-fluoroanthraquinone (9). A mixture of 19.4 g (0.07 mol) of thoroughly dried 1,8-dichloroanthraquinone and 20.0 g (0.13 mol) of anhydrous caesium fluoride in 200 ml of anhydrous dimethyl sulfoxide was heated at 135 °C for 6 h with efficient stirring. The cooled mixture was poured into water and the solid formed was collected by filtration, washed with water and air-dried. Column chromatography of the mixture through alumina with dichloromethane-hexane as the eluent gave 1.37 g (7%) of unreacted 1,8-dichloroanthraquinone, 4.46 g (24%) of 1-chloro-8-fluoroanthraquinone (**9**), and 5.74 g (34%) of 1,8-difluoroanthraquinone[24] in this order. Use of a smaller amount of caesium fluoride would have yielded a larger relative amount of **9**. Recrystallization of the crude **9** from benzene-hexane gave a pure sample of **9**, mp 180—181 °C.

Found: C, 64.43; H, 2.55; Cl, 13.51%. Calcd for $C_{14}H_6ClFO_2$: C, 64.51; H, 2.32; Cl, 13.60%. ^1H NMR δ=7.506 (1H, ddd, J=1.2, 8.3, and 10.7 Hz, 7-H), 7.667 (1H, t, J=7.9 Hz, 3-H), 7.751 (1H, dt, J=4.6 and 8.0 Hz, 6-H), 7.816 (1H, dd, J=1.3 and 8.0 Hz, 2-H), 8.105 (1H, dd, J=1.1 and 7.8 Hz, 5-H), 8.258 (1H, dd, J=1.3 and 7.8 Hz, 4-H). ^{19}F NMR: 50.45 (dd, J=4.8 and 10.4 Hz).

1-Chloro-8-fluoroanthrone (11). A mixture of 2.6 g (10.0 mmol) of **9** and 0.8 g of aluminium powder in 30 ml of concentrated sulfuric acid was stirred at room temperature for 20 h and the mixture was poured onto ice-water. The solid mass was collected by filtration, washed with water, air-dried and extracted with dichloromethane. The ^{19}F NMR of the extract indicated the presence of **11** (48.4 ppm) and 4-chloro-5-fluoroanthrone (44.4 ppm) in a ratio of 6:1. Recrystallization of the mixture from benzene-hexane gave 1.79 g (73%) of spectrally pure **11**, which was used in the subsequent reaction.

^1H NMR δ=4.256 (2H, s, 10-CH_2), 7.090 (1H, dd, J=8.3 and 10.8 Hz, 7-H), 7.192 (1H, d, J=8.1 Hz, 5-H), 7.315 (1H, dd, J=1.6 and 7.3 Hz, 4-H), 7.406 (1H, dd, J=7.3 and 7.9 Hz, 3-H), 7.435 (1H, dd, J=1.6 and 7.9 Hz, 2-H), 7.484 (1H, dt, J=5.0 and 8.0 Hz, 6-H). ^{19}F NMR: 48.43 (dd, J=4.9 and 10.6 Hz).

1,8-Dichloro-9-methylanthracene (12).[8] To an ethereal solution of the Grignard reagent prepared from 4.3 g (30 mmol) of methyl iodide was added 2.63 g (10.0 mmol) of 1,8-dichloroanthrone (**10**),[7] and the mixture was heated under reflux for 1 h, cooled and treated with concentrated hydrochloric acid. The organic layer was washed with water, dried over magnesium sulfate, and concentrated. Chromatography of the residue through an alumina column with hexane as the eluent followed by recrystallization from tetrahydrofuran-hexane gave 1.77 g (68%) of **12**, mp 123—124 °C (lit,[8] 127 °C).

^1H NMR δ=3.387 (3H, s, 9-CH_3), 7.308 (2H, dd, J=7.0 and 8.4 Hz, 3-H and 6-H), 7.593 (2H, dd, J=1.1 and 7.0 Hz, 2-H and 7-H), 7.836 (2H, d, J=8.4 Hz, 4-H and 5-H), 8.234 (1H, s, 10-H).

1-Chloro-8-fluoro-9-methylanthracene (13), mp 78—79 °C, was similarly prepared as above from 1-chloro-8-fluoroanthrone (**11**) in 49% yield.

Found: C, 73.63; H, 4.13; Cl, 14.45%. Calcd for $C_{15}H_{10}ClF$: C, 73.62; H, 4.12; Cl, 14.49%. ^1H NMR δ=3.387 (3H, d, J=7.0 Hz, 9-CH_3), 7.127 (1H, dd, J=7.4 and 14.5 Hz, 7-H), 7.291 (1H, dd, J=7.2 and 8.4 Hz, 3-H), 7.350 (1H, ddd, J=4.7, 7.4, and 8.4 Hz, 6-H), 7.573 (1H, dd, J=1.0 and 7.2 Hz, 2-H), 7.713 (1H, d, J=8.4 Hz, 5-H), 7.830 (1H, d, J=8.4 Hz, 4-H), 8.243 (1H, s, 10-H). ^{19}F NMR: 55.86 (m).

1,8-Dichloro-9-methyltriptycene (6a). To a boiling solution of 261 mg (1.0 mmol) of **12** in 20 ml of 1,2-dimethoxyethane (DME) were added simultaneously a solution of 400 mg (3.0 mmol) of anthranilic acid in 10 ml of DME and a solution of 0.5 ml (ca. 4 mmol) of isopentyl nitrite in 5 ml of DME during the course of 1.5 h. The mixture was heated under reflux for 1 h and concentrated under reduced pressure. The residue was passed through an alumina column with hexane as the eluent to afford 252 mg (75%) of **6a**, mp 338—340 °C (recrystallized from tetrahydrofuran-hexane).

Fooud: C, 74.77; H, 4.28; Cl, 20.88%. Calcd for $C_{21}H_{14}Cl_2$: C, 74.79; H, 4.18; Cl, 21.02%.

8,13-Dichloro-1,2,3,4-tetrafluoro-9-methyltriptycene (6b). To a chilled (−78 °C) solution of 0.4 g (2.0 mmol) of chloropentafluorobenzene in 30 ml of anhydrous diethyl ether was added a 1.5 ml (about 2.5 mmol) of 10% w/v solution of butyllithium in hexane. The solution was stirred at −78 °C for 2 h and 285 mg (1.1 mmol) of powdery **12** was added all at once. The mixture was allowed to slowly warm up to room temperature and then heated under reflux for 3 h. The mixture was washed with water, dried over magnesium sulfate, and concentrated. Column chromatography of the residue through alumina with hexane as the eluent followed by recrystallization from tetrahydrofuran-hexane gave 92 mg (21%) of **6b**, mp 300—301 °C.

Found: C, 61.53; H, 2.63; Cl, 17.71%. Calcd for $C_{21}H_{10}Cl_2F_4$: C, 61.64; H, 2.46; Cl, 17.33%. ^{19}F NMR: 3.28 (app t, J=19 Hz, 2-F), 4.35 (ddd, J=5, 19, and 22 Hz, 3-F), 12.04 (dd, J=15 and 22 Hz, 4-F), 20.70 (br, 1-F).

8,13-Dichloro-1.4-dimethoxy-9-methyltriptycene (6c). A mixture of 448 mg (1.7 mmol) of **12** and 1.08 g (10.0 mmol) of *p*-benzoquinone in 15 ml of acetonitrile was heated under reflux for 2 h. The adduct was obtained as 495 mg (78%) of colorless crystals; ^1H NMR (90 MHz) δ=2.67 (3H, s), 2.94 (1H, d, J=9.3 Hz), 3.20 (1H, dd, J=3.1 and 9.3 Hz), 4.65 (1H, d, J=3.1 Hz), 6.14 (1H, d, J=10.4 Hz), 6.38 (1H, d, J=10.4 Hz), 7.0—7.3 (6H, m).

The adduct was dissolved in 10 ml of dioxane and was treated with 5 ml of 20% aqueous sodium hydroxide and 2 ml of dimethyl sulfate. The mixture was extracted with benzene and the organic layer was washed with water, dried with magnesium sulfate and evaporated to afford 203 mg (38%) of **6c**, mp 343—345 °C, decomp (recrystallized from tetrahydrofuran).

Found: C, 69.30; H, 4.50; Cl, 17.54%. Calcd for $C_{23}H_{18}Cl_2O_2$: C, 69.53; H, 4.57; Cl, 17.85%.

8,13-Dichloro-1,4,9-trimethyltriptycene (6d). To a boiling solution of 261 mg (1.0 mmol) of **12** in 20 ml of DME were added simultaneously a solution of 248 mg (1.5 mmol) of 3,6-dimethylanthranilic acid[25] in 10 ml of DME and a solution of 0.5 ml of isopentyl nitrite in 5 ml of DME during

the course of 2 h. The mixture was heated under reflux for further 1 h. After evaporation of the solvent the residue was passed through alumina with hexane as the eluent. Recrystallization of the eluate from tetrahydrofuran-hexane gave 230 mg (63%) of **6d**, mp 358—360 °C.

Found: C, 75.78; H, 4.96; Cl, 19.18%. Calcd for $C_{23}H_{18}Cl_2$: C, 75.62; H, 4.97; Cl, 19.41%.

1,3-Di-*t*-butyl-8,13-dichloro-9-methyltriptycene (6e). To a boiling solution of 522 mg (2.0 mmol) of **12** in 25 ml of DME were added simultaneously a solution of 750 mg (3.0 mmol) of 3,5-di-*t*-butylanthranilic acid[9b] in 20 ml of DME and a solution of 1.0 ml of isopentyl nitrite in 10 ml of DME during the course of 2 h and the solution was heated under reflux for further 1 h. After evaporation of the solvent the residue was passed through alumina to give a ca. 2:5 mixture of **6e** and the regioisomeric 2,4-di-*t*-butyl derivative (**6f**) in about 85% yield. The isomers were separated using gel permeation chromatography in which **6f** eluted slightly faster. The 1,3-di-*t*-butyl isomer **6e** has a melting point of 251—252 °C (recrystallized from tetrahydrofuran-dichloromethane).

Found: C, 77.66; H, 6.79; Cl, 16.18%. Calcd for $C_{29}H_{30}Cl_2$: C, 77.50; H, 6.73; Cl, 15.77%. The 2,4-di-*t*-butyl isomer **6f** has an mp of 274—275 °C. Found: C, 77.35; H, 6.65; Cl, 15.74%.

8-Chloro-13-fluoro-1,4-dimethoxy-9-methyltriptycene (7a). A mixture of 122 mg (0.5 mmol) of the anthracene **13** and 216 mg (2.0 mmol) of *p*-benzoquinone in 5 ml of acetonitrile was heated under reflux for 20 h to give 126 mg (71%) of the 1:1 adducts. The product was shown to be a mixture of two diastereomers in a ratio of ca. 3:2.

^{1}H NMR (90 MHz, aliphatic protons only); the major isomer: δ=2.52 (3H, d, J=6.9 Hz), 2.92 (1H, d, J=9.2 Hz), 3.21 (1H, dd, J=3.0 and 9.2 Hz), 4.68 (1H, dd, J=2.1 and 3.0 Hz); the minor isomer: δ=2.47 (3H, d, J=6.6 Hz), 2.97 (1H, d, J=9.2 Hz), 3.21 (1H, dd, J=3.2 and 9.2 Hz), 4.71 (1H, dd, J=2.4 and 3.2 Hz). ^{19}F NMR: 47.6 (m, major), 46.5 (m, minor).

The adduct mixture was dissolved in 10 ml of acetic acid containing 0.5 ml of concentrated hydrochloric acid and the solution was stirred at room temperature for 20 h to afford white precipitates. The mixture was poured into water and the solid was collected by filtration, washed with water and air-dried to give crude 8-chloro-13-fluoro-9-methyl-1,4-triptycenediol.

^{1}H NMR (90 MHz, $CDCl_3$-dimethyl sulfoxide 9:1): δ=3.11 (3H, d, J=7.1 Hz), 5.80 (1H, d, J=2.1 Hz), ca. 5.9 (2H, br, OH), 6.3—7.3 (8H, m).

The hydroquinone was dissolved in 30 ml of dichloromethane containing 1.0 ml of dimethyl sulfate and 50 mg of benzyltrimethylammonium chloride, and the mixture was stirred with 20 ml of 10% aqueous potassium hydroxide at room temperature for 20 h. The organic layer was washed with water, dried over magnesium sulfate and concentrated. Column chromatography of the residue through alumina with dichloromethane-hexane (1:4) as the eluent gave 46.8 mg (34%) of **7a**, mp 321—322 °C (recrystallized from tetrahydrofuran-hexane).

Found: C, 72.56; H, 4.58; Cl, 9.26%. Calcd for $C_{23}H_{18}ClFO_2$: C, 72.53; H, 4.76; Cl, 9.31%. ^{19}F NMR: 46.48 (m).

8-chloro-13-fluoro-1,4,9-trimethyltriptycene (7b), mp 316—317 °C (recrystallized from tetrahydrofuran-hexane), was similarly obtained as **6d** in 60% yield from **13** and 3,6-dimethylanthranilic acid.[25]

Found: C, 79.28; H, 4.96; Cl, 10.66%. Calcd for $C_{23}H_{18}ClF$: C, 79.19; H, 5.20; Cl, 10.16%. ^{19}F NMR: 46.58 (m).

Attempted Synthesis of 1,2,3,4-Tetrabromo-8,13-dichloro-9-methyltriptycene (6g). To a boiling solution of 261 mg (1.0 mmol) of **12** in 10 ml of DME were added simultaneously a solution of 906 mg (ca. 2 mmol) of tetrabromoanthranilic acid[26] in 30 ml of DME and a solution of 0.5 ml of isopentyl nitrite in 15 ml of DME during the course of 2 h and the mixture was heated under reflux for further 0.5 h. Evaporation of the solvent afforded yellowish solids which were hardly soluble in common solvents. ^{1}H NMR ($CDCl_3$) of the supernatant solution showed a small broad peak at δ=3.50 presumably ascribable to the 9-methyl protons of **6g** together with many large signals due to more soluble impurities. Further characterization and purification of **6g** was abandoned.

Lineshape Analysis of the Dynamic NMR Spectra. For each compound, the slow exchange limit spectra at several temperatures were iteratively simulated using the LAOCN3 program[10] to obtain the NMR parameters. Coupling constants were independent of temperature, but chemical shifts were generally temperature dependent. Exchange-broadened spectra at intermediate temperatures were simulated by visual matching using the DNMR3 program.[11] Chemical shifts at each temperature were obtained by linear extrapolation of the slow exchange limit data. The T_2 values were properly adjusted judging from the half-width of the TMS signal.

Molecular Mechanics Calculations. Calculations were performed using the BIGSTRN-3 program.[13] As the program does not contain parameters for halogen atoms attached to a benzene ring, necessary parameters[27] were added as compiled in Table 6. The van der Waals parameters for H and C(sp^2) and the dipole moments for C(sp^2)-H and

Table 6. Modified and Added Force Field Parameters[a,b]

Stretching	K_s/mdyn Å^{-1}	r_o/Å	μ/D
1-30			0.9
5-30			0.6
11-30	6.1	1.35	−1.66
12-30	3.7	1.74	−1.78

Bending	K_b/mdyn rad^{-1}	θ_o/°
11-30-30	0.97	120.0
12-30-30	0.83	119.0

Torsion	V_3/kcal mol^{-1}
11-30-30-30	15.0
11-30-30-11	15.0
1-30-30-11	15.0
5-30-30-11	15.0
12-30-30-30	15.0
1-30-30-12	15.0
5-30-30-12	15.0
5- 1 -1-30	0.0

van der Waals	r/Å	ε
5	1.62	0.020
30	1.96	0.056

a) Atom type: 1, sp^3-C; 5, H; 11, F; 12, Cl; 30, sp^2-C.
b) 1 mdyn Å^{-1}=10^2 N m^{-1}, D=Debye (1 D=3.3356×10^{-30} C m).

$C(sp^2)$-$C(sp^3)$ bonds were modified.[28] The torsional parameter V_3 for $C(sp^2)$-$C(sp^3)$-$C(sp^3)$-H was altered as recommended by Imashiro et al.[14c]

References

1) Part LIX : G. Yamamoto and M. Ōki, *Bull. Chem. Soc. Jpn.*, **59**, 3597 (1986).

2) a) M. Nakamura, M. Ōki, and H. Nakanishi, *J. Am. Chem. Soc.*, **95**, 7169 (1973); b) See also: J. E. Anderson and D. I. Lawson, *J. Chem. Soc., Chem. Commun.*, **1973**, 830.

3) M. Nakamura, M. Ōki, H. Nakanishi, and O. Yamamoto, *Bull. Chem. Soc. Jpn.*, **47**, 2415 (1974).

4) W. D. Hounshell, L. D. Iroff, D. J. Iverson, R. J. Wroczynski, and K. Mislow, *Isr. J. Chem.*, **20**, 65 (1980).

5) a) G. Yamamoto, M. Suzuki, and M. Ōki, *Angew. Chem., Int. Ed. Engl.*, **20**, 607 (1981); *Bull. Chem. Soc. Jpn.*, **56**, 306 (1983); b) G. Yamamoto, M. Suzuki, and M. Ōki, *Chem. Lett.*, **1980**, 1523; *Bull. Chem. Soc. Jpn.*, **56**, 809 (1983); c) G. Yamamoto and M. Ōki, *ibid.*, **56**, 2082 (1983).

6) A part of the results has been published : G. Yamamoto and M. Ōki, *Tetrahedron Lett.*, **26**, 457 (1985).

7) E. de B. Barnett and M. A. Matthews, *J. Chem. Soc.*, **123**, 2549 (1923).

8) E. de B. Barnett, N. F. Goodway, and J. L. Wiltshire, *Ber. Dtsch. Chem. Ges.*, **63**, 472 (1930).

9) See for example: a) G. Yamamoto and M. Ōki, *Bull. Chem. Soc. Jpn.*, **59**, 3597 (1986); b) R. W. Franck and E. G. Leser, *J. Org. Chem.*, **35**, 3932 (1970); c) J. E. Anderson, R. W. Franck, and W. L. Mandella, *J. Am. Chem. Soc.*, **94**, 4608 (1972).

10) A. A. Bothner-By and S. M. Castellano, QCPE Program No. 111.

11) D. A. Kleier and G. Binsch, QCPE Program No. 165.

12) e.g., Y. Kawada and H. Iwamura, *J. Am. Chem. Soc.*, **105**, 1449 (1983).

13) R. B. Nachbar, Jr. and K. Mislow, QCPE Program No. 514.

14) a) F. Imashiro, T. Terao, and A. Saika, *J. Am. Chem. Soc.*, **101**, 3762 (1979); b) F. Imashiro, K. Takegoshi, T. Terao, and A. Saika, *ibid.*, **104**, 2247 (1982); c) F. Imashiro, K. Hirayama, K. Takegoshi, T. Terao, and A. Saika, *J. Chem. Soc., Perkin Trans. 2*, **1988**, 1401.

15) a) L. Pauling, "The Nature of the Chemical Bond," 3rd ed, Cornell Univ. Press, New York (1960), p 260; b) M. Charton, *J. Am. Chem. Soc.*, **91**, 615 (1969); c) G. Bott, L. D. Field, and S. Sternhell, *ibid.*, **102**, 5618 (1980).

16) See Ref. 4 and also: H. Förster and F. Vögtle, *Angew. Chem., Int. Ed. Engl.*, **16**, 429 (1977).

17) G. Yamamoto and M. Ōki, *Bull. Chem. Soc. Jpn.*, **58**, 1690 (1985).

18) Analysis of the ^1H-^{13}C COSY spectrum of **6b** at ambient temperature indicates that the coupling constant of the 9-methyl protons with 1-F is of the same sign as that of the 9-methyl carbon with 1-F which is considered to be positive: Dr. I. D. Rae, Monash University, Australia, private communication.

19) This idea was previously suggested by Jefford et al. to explain the significant H-F coupling in a tricyclo-[3.2.1.$0^{2,4}$]octane compound: C. W. Jefford, D. T. Hill, L. Gosez, S. Toppet, and K. C. Ramey, *J. Am. Chem. Soc.*, **91**, 1532 (1969).

20) S. Winstein, P. Carter, F. A. L. Anet, and A. J. R. Brown, *J. Am. Chem. Soc.*, **87**, 5247 (1965).

21) G. Izumi, G. Yamamoto, and M. Ōki, *Bull. Chem. Soc. Jpn.*, **54**, 3064 (1981).

22) Y. Tamura, H. Takizawa, G. Yamamoto, and M. Ōki, *Bull. Chem. Soc. Jpn.*, **63**, 2555 (1990).

23) H. Duddeck, *Top. Stereochem.*, **16**, 219 (1986).

24) G. Yamamoto and M. Ōki, *Bull. Chem. Soc. Jpn.*, **54**, 473 (1981).

25) S. Gronowitz and G. Hansen, *Ark. Kemi*, **27**, 145 (1967).

26) H. Heaney, K. G. Mason, and J. M. Sketchley, *J. Chem. Soc. C*, **1971**, 567.

27) K. Tanabe, S. Tsuzuki, T. Uchimaru, and E. Ōsawa, *Chem. Express*, **3**, 591 (1988).

28) N. L. Allinger and J.-H. Lii, *J. Comput. Chem.*, **8**, 1146 (1987); J.-H. Lii and N. L. Allinger, *J. Am. Chem. Soc.*, **111**, 8576 (1989).